ELSEVIER

Journal of Alloys and Compounds 446–447 (2007) 173–177

Journal of ALLOYS AND COMPOUNDS

www.elsevier.com/locate/jallcom

H-sorption behaviour of mechanically activated Mg–Zn powders

Stefano Deledda [a,*], Bjørn C. Hauback [a], Helmer Fjellvåg [b]

[a] *Physics Department, Institute for Energy Technology, P.O. Box 40, NO-2027 Kjeller, Norway*
[b] *Chemistry Department, University of Oslo, P.O. Box 1033 Blindern, NO-0318 Oslo, Norway*

Received 31 October 2006; accepted 29 November 2006
Available online 29 December 2006

Abstract

We report here on powder mixtures, with nominal compositions Mg_7Zn and Mg_7Zn_3, which were ball milled (i) at room temperature in an inert Ar atmosphere, (ii) at liquid nitrogen temperature (cryomilling), and (iii) at room temperature in a reactive H_2 atmosphere (reactive milling). In all cases, ball milling results in the formation of an amorphous Mg–Zn phase with a likely composition of about $Mg_{45}Zn_{55}$. A fraction of Mg is left unreacted and transforms to MgH_2 if ball milling is carried out in a reactive H_2 atmosphere. Hydrogen-absorption (H-absorption) in a Sievert-type apparatus for the powders ball milled in Ar results in the partial conversion of the Mg into MgH_2. The amorphous Mg–Zn phase appears not to play any significant role in the hydrogen-sorption (H-sorption) behaviour and crystallizes into $Mg_{21}Zn_{25}$. The latter partially decomposes into MgH_2 and $MgZn_2$, provided the hydrogenation reaction is extended for sufficiently long times.

Keywords: Hydrogen storage materials; High-energy ball milling

1. Introduction

Ball milling techniques are recognized as an important tool for processing potential Mg-based hydrogen storage materials. On one hand, this is due to the grain-size reduction process, which occurs during the continuous fracturing and cold welding of the powder particles and resulting in an improved hydrogen-sorption (H-sorption) kinetics [1]. On the other hand, the mixing of elements/compounds at an atomic scale and the extended solid solubility of metals, which is observed upon ball milling, allows the production of metastable alloys with possible interesting hydrogen storage properties [2]. We have therefore investigated the effect of ball milling on the hydride-formation processes in the Mg–Zn system.

It was previously reported by Bruzzone et al. [3] that the $Mg_{51}Zn_{20}$ intermetallic compound obtained by annealing elemental powder mixtures could absorb up to 3.62 wt%. The resulting hydrogenated compound corresponded to a nominal composition of $Mg_{51}Zn_{20}H_{95}$. However, Song and Park [4] later pointed out that, upon hydrogenation, $Mg_{51}Zn_{20}$ decomposes into Mg and other Mg–Zn intermetallic compounds, and Mg is the only species taking part in the hydriding/dehydriding process. More recently, Jonsson [5] calculated with a density functional theory (DFT) approach the stability and hydrogen-release temperature for Mg–TM hydrides (TM = 3d transition metals) having a nominal composition Mg_7TMH_x and an fcc-like structure. They reported that Mg_7ZnH_{16} whose formation is thermodynamically possible, is expected to desorb hydrogen at temperatures close to room temperature. The dissociation into the elements or into the dehydrogenated Mg_7Zn alloy was shown to be equally favorable.

In this work, we have explored the possibility to synthesize novel Mg–Zn ternary hydrides with interesting hydrogen storage properties by ball milling (i) at room temperature in an inert Ar atmosphere, (ii) at liquid nitrogen temperature (cryomilling), and (iii) at room temperature in a reactive H_2 atmosphere (reactive milling). The investigation was focused on two Mg-to-Zn molar ratios: 7:1 (based on the predicted existence of the hydride Mg_7ZnH_{16} from the DFT calculations) and 51:20 (corresponding to the only Mg-rich intermetallic compound, $Mg_{51}Zn_{20}$, reported in the Mg–Zn phase diagram [6] and whose H-sorption properties were previously investigated).

2. Experimental

Elemental powder mixtures with nominal composition Mg_7Zn and $Mg_{51}Zn_{20}$ were ball milled using either a Fritsch P6 planetary ball mill or a SPEX 6750 Freezer/Mill. The latter allows milling to be carried out at liquid

* Corresponding author.
E-mail address: stefano.deledda@ife.no (S. Deledda).

0925-8388/$ – see front matter © 2006 Elsevier B.V. All rights reserved.
doi:10.1016/j.jallcom.2006.11.189

nitrogen temperature (cryomilling). All the powders were handled in a glove box under a protecting Ar atmosphere. For the planetary mill, stainless vials, and balls were used. The ball-to-powder ratio was about 40:1 and the rotational velocity was set to 400 rpm. A modified lid equipped with a valve for the introduction of gases in the volume of the vial allowed milling also in a H_2 atmosphere at 5.5 bar. In such cases, H_2 was refilled periodically each 10 h of milling. Cryomilling was performed using a specially designed stainless steel vial, in order to minimize oxygen and nitrogen contaminations, and with a stainless steel cylindrical impactor. The mass ratio between the impactor and the powder was 15:1.

The powders ball milled in Ar were subsequently hydrogenated at 575 K and an initial pressure of about 80 bar in a Sievert-type apparatus designed and built in-house at IFE. The hydrogen-containing samples were analyzed by thermal desorption spectroscopy (TDS), which was carried out in dynamic vacuum at a heating rate of 2 K/min up to 575 K.

Powder X-ray diffraction (PXD) was carried out using an INEL MPD diffractometer and a Siemens D5000 diffractometer both with Cu Kα radiation. Selected samples were analyzed at the Swiss–Norwegian beam line (BM1A) at the European Synchrotron Radiation Facility (ESRF) in Grenoble, France. Scanning electron microscopy (SEM) was performed using a Hitachi S-4800 equipped with a cold field emission electron source.

3. Results and discussion

3.1. Ball milling in Argon

Fig. 1 shows the PXD patterns for Mg–Zn powders after ball milling in Ar. After 50 h of milling in a planetary ball mill, a broad diffraction maximum centred at $Q \approx 2.71$ Å^{-1} can be observed for both the Mg_7Zn (pattern a) and $Mg_{51}Zn_{20}$ powders (pattern b). This suggests the formation of an amorphous phase. At the same time diffraction peaks from elemental Mg are superimposed on the broad diffraction maximum, indicating that a significant fraction of Mg is left unreacted. No structural changes are detected if the milling time is increased to 100 h (see pattern c for the $Mg_{51}Zn_{20}$ powder). In Fig. 1d the PXD pattern for as-milled $Mg_{51}Zn_{20}$ mixture after 9 h of cryomilling is shown. Also in this case peaks from elemental Mg are superimposed on a broad diffraction maximum centred at $Q \approx 2.71$ Å^{-1}. Hence, despite the relative short milling time in this case, the formation of an amorphous phase can be assumed to occur also upon cryomilling.

The diffraction peaks for the unreacted magnesium have about the same intensity in all patterns, except in the pattern for Mg_7Zn, that is the system richer in Mg, which are considerably more intense. This suggests that the amorphous phase, which forms upon mechanical alloying, has about the same composition regardless the nominal composition of the initial elemental powder mixtures. More Mg in the system gives more unreacted magnesium. Furthermore, we can assume the composition of the amorphous phase to be of around $Mg_{45}Zn_{55}$ (at.%). For this composition Miedema semi-empirical model predicts a minimum in the enthalpy of formation of an Mg–Zn amorphous phase, as reported by Calka and Radlinsky [7] They have also investigated the amorphization of Mg–Zn alloys upon mechanical alloying and found that a complete amorphization was not achieved when pure $Mg_{70}Zn_{30}$ elemental powders were mechanically alloyed for up to 100 h.

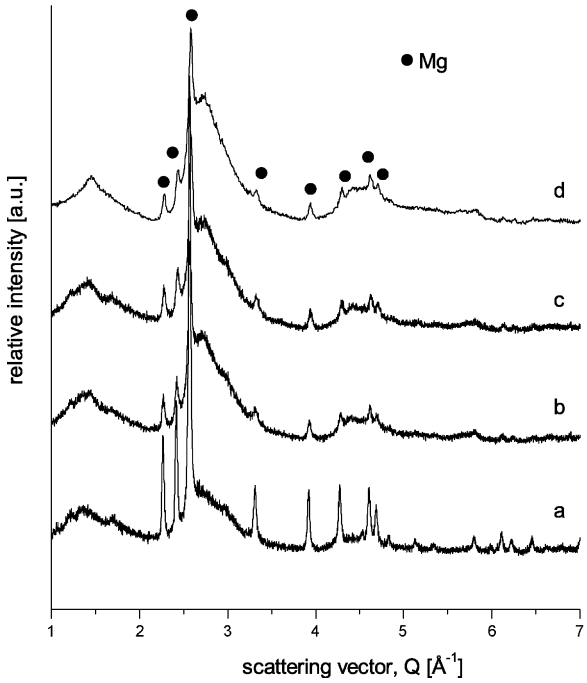

Fig. 1. PXD patterns for (a) Mg_7Zn ball milled for 50 h in Ar using a planetary mill, (b) $Mg_{51}Zn_{20}$ ball milled for 50 h in Ar using a planetary mill, (c) $Mg_{51}Zn_{20}$ ball milled for 100 h in Ar using a planetary mill, and (d) $Mg_{51}Zn_{20}$ cryomilled for 9 h.

The powders ball milled in Ar atmosphere were hydrogenated in a Sievert-type apparatus. The amount of hydrogen absorbed by each sample is summarized in Table 1 together with the temperature and initial pressure at which hydrogenation was performed. In Fig. 2 the PXD patterns for the absorption products are shown. The sample with the highest relative content of magnesium, Mg_7Zn, was the one that absorbed most hydrogen, that is 4.4 wt% after 92 h at 574 K. As shown by PXD analysis (Fig. 2c) the powder after hydrogenation consists of a mixture of tetragonal MgH_2 (main phase), $MgZn_2$, $Mg_{21}Zn_{25}$, and Mg. The planetary ball milled $Mg_{51}Zn_{20}$ powders absorbed 1.3 wt% H_2 after 5 h at 585 K, whereas the cryomilled powders with the same composition absorbed 0.2 wt% H_2 after 18 h at

Table 1
Absorption data (H/Mg and gravimetric capacity) for Mg–Zn powders. Some experimental conditions, that is temperature, initial pressure, and absorption time, are also given

	Temperature (K)	Initial pressure (bar)	Time (h)	H/Mg	wt%
Ball milled $Mg_{51}Zn_{20}$	585	79.3	5	0.63	1.3
Cryomilled $Mg_{51}Zn_{20}$	563	82.4	18	0.09	0.2
Ball milled Mg_7Zn	574	78.6	92	1.47	4.4

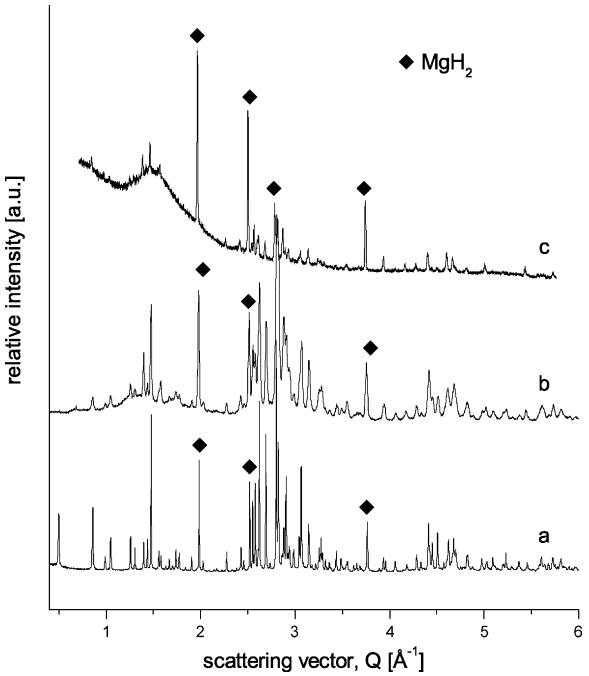

Fig. 2. PXD patterns after hydrogenation for (a) $Mg_{51}Zn_{20}$ ball milled for 100 h in a planetary mill, (b) cryomilled $Mg_{51}Zn_{20}$, and (c) Mg_7Zn ball milled for 50 h in a planetary mill. To avoid confusion only the diffraction peaks from MgH_2 are marked, the remaining reflections stemming from $Mg_{21}Zn_{25}$, $MgZn_2$, and Mg.

563 K. Also in these cases the only hydrogen-containing phase detected by PXD after hydrogenation was tetragonal MgH_2 (see Fig. 2a and b, respectively). The main phase is $Mg_{21}Zn_{25}$ and diffraction peaks from elemental Mg and $MgZn_2$ can also be observed.

Absorption experiments and PXD data suggest that the species that undergoes hydrogenation is metallic Mg, resulting in the formation of MgH_2. On the other hand, the amorphous Mg–Zn phase, which is observed after ball milling, seems not to play an active role and crystallizes most likely into Mg–Zn intermetallic compounds. As previously reported for melt-spun ribbons with composition close to the eutectic [8], Mg–Zn glasses usually crystallize at temperatures as low as 350 K. In particular, above 500 K the crystallization of amorphous $Mg_{60}Zn_{40}$ results in the formation of Mg and "MgZn". (The accurate stoichiometry for the intermetallic compound MgZn was later reported together with its crystalline structure as $Mg_{21}Zn_{25}$ [9]). In our case, this suggests that, when the powders are heated up above 550 K for hydrogenation, the amorphous phase produced by ball milling and assumed composition around $Mg_{45}Zn_{55}$, crystallizes into $Mg_{21}Zn_{25}$, corresponding to $Mg_{45.6}Zn_{54.4}$ at.%.

Furthermore, PXD data show that also $MgZn_2$ forms during hydrogenation. This indicates that upon hydrogenation $Mg_{21}Zn_{25}$ partially decomposes into MgH_2 and $MgZn_2$. Accordingly, the quantity of the hydrogen absorbed by the ball milled Mg–Zn powders is governed not only by the relative content of magnesium, but also by the time of the hydrogenation reaction. This would explain why the amount of hydrogen absorbed by the Mg_7Zn sample is significantly larger than that absorbed by the $Mg_{51}Zn_{20}$ ball milled powders (Table 1). On the other hand, the small capacity observed for the $Mg_{51}Zn_{20}$ cryomilled powder likely stems from the relatively low reaction temperature, that is 563 K compared to 585 K for planetary milled $Mg_{51}Zn_{20}$, and the resulting slower hydrogen-absorption (H-absorption) kinetics.

3.2. Ball milling in hydrogen

Fig. 3 shows the PXD patterns for the $Mg_{51}Zn_{20}$ and Mg_7Zn powders ball milled in H_2 atmosphere at 5.5 bar for different milling times. For the $Mg_{51}Zn_{20}$ system, patterns a to c show that the milling produces an amorphous phase already after 20 h, and a large fraction of Mg is left unreacted. The broad diffraction maximum associated with the amorphous phase is observed at $Q \approx 2.70\ Å^{-1}$. This is nearly identical to the value observed for the powders ball milled in Ar. After 40 h of milling (Fig. 3b) the 110 ($2\theta \approx 27°$) and 211 ($2\theta \approx 55°$) reflections of MgH_2 can be observed, and at the same time the intensity of the Mg peaks decrease. This suggests that the hydride forms at the expenses of the Mg. More MgH_2 forms when the milling time is increased to 60 h (Fig. 3c), although not all Mg is transformed. In addition, the amorphous maximum sharpens, indicating that a nanocrystalline phase, likely $Mg_{51}Zn_{20}$, is precipitating from the amorphous phase. For the Mg_7Zn powders, Mg is observed as the main phase after 40 h (Fig. 3d). However, the relatively high intensity of the 110 reflection for MgH_2 points out that a significant fraction of Mg has been hydrated. Moreover, the partial precipitation of nanocrystalline $Mg_{21}Zn_{25}$ is observed as the amorphous halo sharpens. Extending the milling time up to 100 h (Fig. 3e) results in the almost complete conversion of

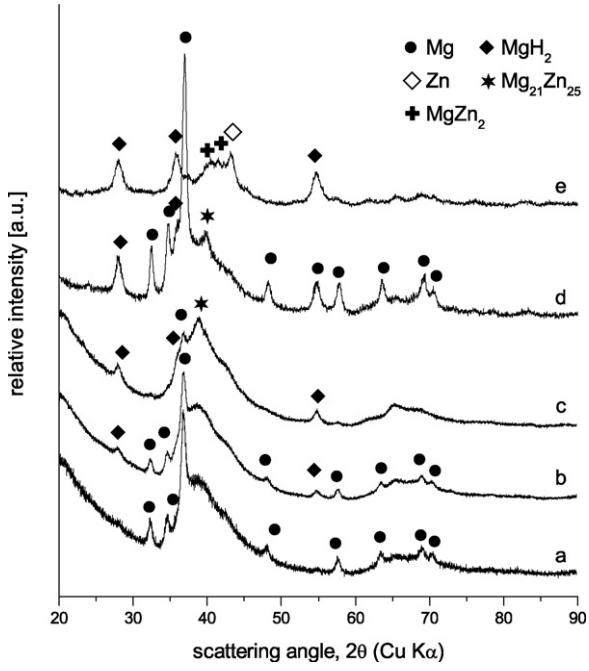

Fig. 3. PXD patterns (Cu Kα) for $Mg_{51}Zn_{20}$ and Mg_7Zn after reactive milling in H_2 for (a) 20 h, (b) 40 h, (c) 60 h, and (d) 40 h, (e) 100 h, respectively.

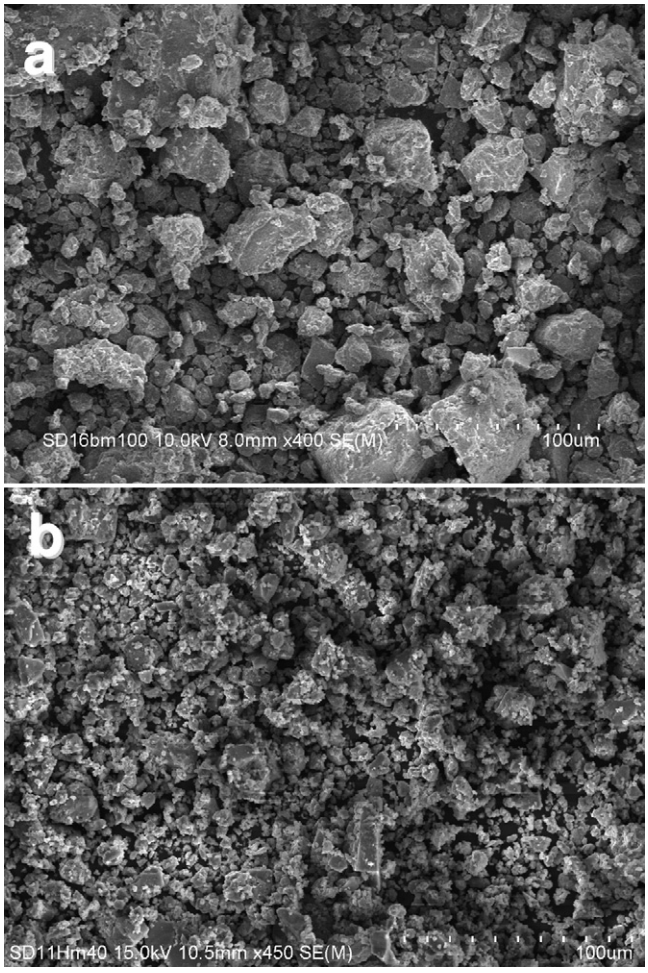

Fig. 4. Secondary-electron SEM images for $Mg_{51}Zn_{20}$ (a) ball milled for 100 h in Ar using a planetary mill and (b) ball milled for 60 h in H_2.

elemental Mg into MgH_2. At the same time broad diffraction peaks from $MgZn_2$ and metallic Zn can be observed.

According to the PXD data, the hydrogenation reaction occurring upon reactive milling in hydrogen can be regarded as analogous to that discussed above for the powders milled in argon and hydrogenated at about 575 K and 80 bar. MgH_2 forms first from unreacted elemental Mg after the amorphization reaction. When most of the "free" magnesium is consumed, MgH_2 starts to form at the expenses of $Mg_{21}Zn_{25}$. The latter precipitates from the amorphous phase and decomposes to MgH_2 and $MgZn_2$. It is worth noticing that in this case, that is by reactive milling, the crystallization of the amorphous phase is triggered by the combined action of the mechanical treatment and H_2 rather than by temperature as observed above. Furthermore, ball milling in a hydrogen atmosphere promotes the reduction of the particle size. This is shown in Fig. 4, which compares the secondary-electron SEM images for $Mg_{51}Zn_{20}$ powders (a) ball milled in Ar for 100 h and (b) ball milled in H_2 for 60 h. It can be observed that after ball milling in argon the average particle size can be estimated around 20 μm. Some particles are as large as 60 μm. After reactive milling the particles are smaller than 5 μm, and most are around 1 μm.

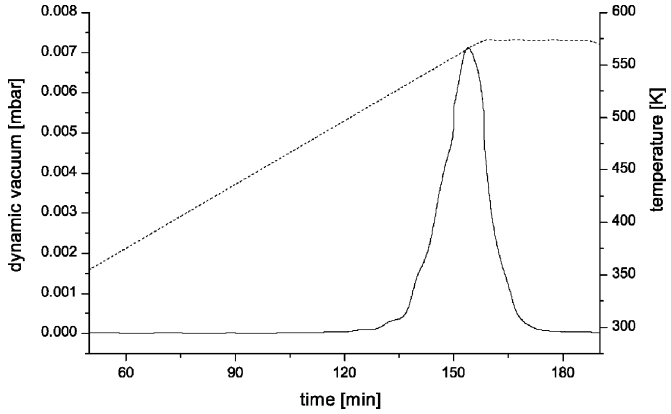

Fig. 5. TDS curve for $Mg_{51}Zn_{20}$ ball milled for 60 h in H_2. The dashed line refers to the temperature ramp (2 K/min).

Finally, TDS was carried out for the $Mg_{51}Zn_{20}$ powders after reactive milling. Fig. 5 shows that desorption sets is at about 525 K and proceeds in one step. The desorption peak is likely related to the desorption of MgH_2. The relative low desorption temperature is due to both the effect of ball milling and the possible catalytic action of Zn [1]. Indeed, the only phases detected by the PXD analysis after TDS (not shown) are $Mg_{21}Zn_{25}$ (main phase), Mg and MgH_2. The presence of residual MgH_2 indicates that the desorption is only partial and suggests that temperatures higher than 575 K are required to achieve a full conversion from MgH_2 to Mg. Moreover, it is worth noticing that no diffraction peaks from $MgZn_2$ were observed by PXD after TDS. This confirms that the Mg–Zn amorphous phase crystallizes polymorphously to $Mg_{21}Zn_{25}$, and that $MgZn_2$ forms as a result of the H_2-driven decomposition of $Mg_{21}Zn_{25}$.

4. Conclusions

Ball milling of $Mg_{21}Zn_{25}$ and Mg_7Zn powder mixtures results in the formation of an amorphous Mg–Zn phase with a likely composition of about $Mg_{45}Zn_{55}$. A fraction of Mg is left unreacted and transforms to MgH_2 if ball milling is carried out in a reactive H_2 atmosphere. Hydrogen desorption for the reactively milled powders sets in at about 525 K. However, temperatures above 575 K should be reached to have complete desorption. Hydrogen-absorption for the powders ball milled in Ar results in the partial conversion of the Mg into MgH_2. In all cases, the amorphous Mg–Zn phase appears not to play any significant role in the H-sorption behaviour and crystallizes into $Mg_{21}Zn_{25}$. The latter partially decomposes into MgH_2 and $MgZn_2$, provided the hydrogenation reaction is extended for sufficiently long times.

Acknowledgements

The authors would like to thank H. Jónsson for stimulating discussions on the DFT results. The RENERGI Program of Research Council of Norway is gratefully acknowledged for financial support. The skilful assistance from the project team

at the Swiss–Norwegian beam line, ESRF, is also gratefully acknowledged.

References

[1] A. Zaluska, L. Zaluski, J.O. Ström-Olsen, J. Alloys Compd. 288 (1999) 217–225.
[2] Y. Zhang, Y. Tsushio, H. Enoki, E. Akiba, J. Alloys Compd. 393 (2005) 147–153.
[3] G. Bruzzone, G. Costa, M. Ferretti, G.L. Olcese, Int. J. Hydrogen Energy 8 (1983) 459–461.
[4] M.Y. Song, H.R. Park, Int. J. Hydrogen Energy 18 (1993) 653–660.
[5] H. Jonsson, Presented at the International Symposium on Metal–Hydrogen Systems, MH2006, October 1–6, 2006, Lahaina, Maui, Hawaii.
[6] J.B. Clark, L. Zabdyr, Z. Moser, in: A.A. Nayeb-Hashemi, J.B. Clark (Eds.), Phase Diagrams of Binary Mg-Alloys, ASM International, Materials Park, OH, 1988, pp. 353–364.
[7] A. Calka, A.P. Radlinski, Mater. Sci. Eng. A 118 (1989) 131–135.
[8] Z. Altounian, Tu Guo-Hua, J.O. Strom-Olsen, J. Mater. Sci. 17 (1982) 3268–3274.
[9] R. Černy, G. Renaudin, Acta Crystallogr. C58 (2002) i154–i155.